

Complex Iridium(III) Salts: Luminescent Porous Crystalline Materials**

Matteo Mauro, Klaus C. Schuermann, Roger Prôtôt, Andreas Hafner, Pierluigi Mercandelli, Angelo Sironi, and Luisa De Cola*

Dedicated to Jean-Pierre Sauvage on the occasion of his 65th birthday

Iridium(III) complexes have been widely explored in recent years because of their outstanding photophysical properties and superior photo- and chemical stability.^[1–4] Much effort has been devoted to both neutral and cationic luminescent iridium complexes in which fine tuning of the energy of their long-lived excited state can be achieved by proper choice of the coordinated ligands.^[5–9] Furthermore, their excited states can be populated by a charge recombination reaction upon injection of holes and electrons in a simple optoelectronic device, which has resulted in an incredible development within the field of phosphorescent organic light-emitting diodes (OLEDs) and light-emitting electrochemical cells (LEECs).^[10–14] To date, these devices are the most promising for large-area displays and for replacing bulb-based lighting technology.^[15–17] Currently, the fundamental colors (red, green, and blue) needed to obtain white-light emitting devices are based on the emission of individual neutral iridium complexes evaporated on top of each other. However, some papers report the photophysical behavior of multi-component, covalently linked systems containing different emitting complexes.^[18–20] Almost all of these systems involve

partial energy transfer from a larger-band-gap energy donor (blue emitter) to a smaller-band-gap energy acceptor (orange-red emitter). Common device architectures rely on amorphous materials, owing to the better miscibility of the materials with polymeric matrices as well as better film formation properties. Designing systems in which these parameters are fixed offers an alternative approach that permits greater control over the energy transfer processes between donor and acceptor moieties.

On the other hand, a strong effort is devoted to the development of luminescent crystalline organometallic frameworks as well as coordination polymers to obtain 1D and 3D ordered materials in which the metals play a fundamental role in the structure formation as well as in the spectroscopic properties of the crystalline material. Moreover, several examples of porous organic–inorganic hybrid materials made by organosilica are known. In these cases it is also possible to insert luminescent organic or organometallic groups into the pore walls, thus resulting in materials having functional frameworks.^[21,22]

Most of these structures involve strong covalent interactions such as coordination bonds to a mono- or multinuclear metal center, as in metal–organic frameworks (MOFs),^[23–25] but examples consisting of weaker noncovalent interactions are known.^[26] The latter are usually formed from purely organic compounds linked by hydrogen bonds, and the individual building blocks are commonly referred to as tectons. Furthermore, among nano- and meso-sized porous materials, zeolites surely represent one of the most interesting platforms for constructing materials for optical applications. Indeed, when the pores are filled with dyes or light-emitting polymers, an optically active doped material is obtained.^[27,28]

To our knowledge, no crystalline porous systems with luminescent iridium complexes have been reported to date, and there are no reports of luminescent crystalline complexes formed by two metal complexes that are simply the counterion of each other.

Herein we report a new class of materials in which two luminescent iridium complexes, which possess different emission colors and complementary charges, are employed to form complex salts and noncovalently linked crystalline porous frameworks. This strategy can be extended to many photo- and electroresponsive ionic transition-metal complexes and could constitute the future generation of organometallic zeolite-like structures.

Our complex salts are formed by blue- or green-emitting anionic iridium species and yellow- or red-orange-emitting

[*] K. C. Schuermann, Prof. Dr. L. De Cola
Physikalisches Institut und Center for Nanotechnology (CeNTech)
Westfälische Wilhelms-Universität Münster
Mendelstrasse 7, 48149 Münster (Germany)
Fax: (+49) 251-980-2834
E-mail: decola@uni-muenster.de
Homepage: <http://www.uni-muenster.de/Physik.PI/DeCola>

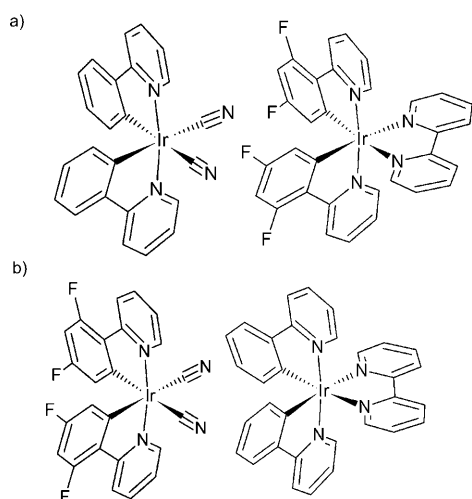
M. Mauro
Dipartimento di Chimica Inorganica, Metallorganica ed Analitica
“L. Malatesta” and INSTM Udr di Milano
Università degli Studi di Milano
Via G. Venezian 21, 20133 Milano (Italy)

Dr. R. Prôtôt, Dr. A. Hafner
Ciba Inc., Group Research, 4002 Basel (Switzerland)

Dr. P. Mercandelli, Prof. A. Sironi
Dipartimento di Chimica Strutturale e Stereochimica Inorganica
and INSTM Udr di Milano
Università degli Studi di Milano
Via G. Venezian 21, 20133 Milano (Italy)

[**] M.M. thanks Regione Lombardia and European Social Found for founding the fellowship “Borse di ricerca applicata per studenti di dottorato” and Ciba Inc., Basel (CH), Research Group for housing. Dr. Federico Polo is kindly acknowledged for preliminary cyclic voltammetric measurements. Universität Münster is kindly acknowledged.

Supporting information for this article is available on the WWW under <http://dx.doi.org/10.1002/anie.200905713>.



Scheme 1. Luminescent complex salts: a) **1**, b) **2**.

cationic iridium complexes (Scheme 1). We are able to precipitate the salts as crystalline materials. A single-crystal structure of one of them shows that they form fascinating 3D porous networks (Figure 1; see Figure S1 in the Supporting Information for the a view of the structure with probability ellipsoids). Furthermore, the emission properties of the salts can be modulated by inclusion of a solvent or by inserting small molecules inside the channels.^[29]

The complex salts reported herein were prepared using a special strategy to eliminate the nonluminescent counterions that balance the negative or positive charges of the emitting complexes. To enhance the tendency to obtain crystalline porous materials, a number of characteristics have been incorporated into the building blocks. Firstly, the complexes have similar geometries (in this case octahedral, D_3 symmetry) to simplify crystal packing, they have equal and opposite net charges (± 1), they are substituted with fluorine groups to promote halogen–hydrogen interactions, and they possess small counterions, which may yield easily removable water-soluble salts once the metal complexes are combined (Scheme 1). The emission color and high emission quantum yields are also parameters that have been taken into account for the network construction. We have combined the cationic compounds $[\text{Ir}(\text{dfppy})_2(\text{bpy})]\text{Cl}$ (**1a**) and $[\text{Ir}(\text{ppy})_2(\text{bpy})]\text{Cl}$ (**2a**; dfppy = 4,6-difluorophenylpyridine, ppy = 2-phenylpyridine, and bpy = 2,2'-bipyridine), previously reported by our group,^[18] with the anionic complexes $(\text{NBu}_4)[\text{Ir}(\text{ppy})_2(\text{CN})_2]$ (**1b**) and $\text{K}[\text{Ir}(\text{dfppy})_2(\text{CN})_2]$ (**2b**).^[12] The counterions of the metal complexes were selected to obtain, as resulting salts, either the water-soluble KCl or the almost water-insoluble salt NBu_4Cl . In the latter case, the extraction of the NBu_4Cl species can be followed by ^1H NMR spectroscopy.

Successful quantitative synthesis of the double iridium complexes starts from strictly equimolar amounts of the two luminescent components in dichloromethane. The water-soluble non-emitting salts are selectively extracted with water, and the corresponding double-complex salts are obtained in very good yields as bright yellow or orange-yellow microcrystalline powders from the dichloromethane

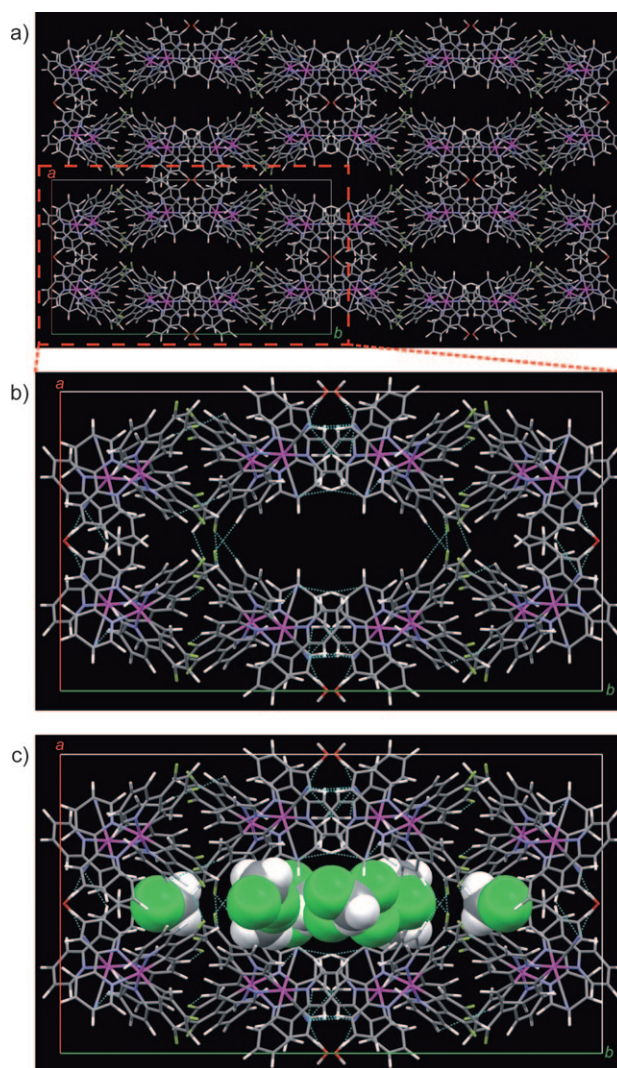


Figure 1. a) Crystal packing of the double complex salt **1**. Four unit cells are represented, and for clarity all solvent molecules are eliminated. The picture highlights the channels running along the c axis. b) Enlarged representation of one unit cell. c) Enlarged representation of one unit cell; the solvent dichloromethane molecules inside the channels and pockets are highlighted with a space-filling representation.

solution by precipitation with ethyl acetate and diethyl ether. Finally, to obtain spectroscopically pure samples, they were recrystallized according to the procedure in the Supporting Information. The purity of the obtained compounds was checked by ^1H and ^{19}F NMR spectroscopy, high-resolution mass spectrometry, and elemental analysis.

One of these new luminescent compounds (**1**) was crystallized and the structure analyzed by means of single-crystal X-ray diffraction.^[30] In addition to the luminescent complexes, the structure contains water and dichloromethane solvate molecules in a 2:1:5 ratio. Water molecules bridge pairs of anions by $\text{C}\equiv\text{N}\cdots\text{H}-\text{O}-\text{H}\cdots\text{N}\equiv\text{C}$ hydrogen bonds. A pattern of weak interactions can be also detected: $\text{C}-\text{H}\cdots\pi(\text{C}\equiv\text{N})$ hydrogen bonds between anions and cations, $\text{C}-\text{H}\cdots\text{F}$ hydrogen bonds between cations, and π -stacking interactions between the pyridine and the phenyl moieties of bipyridine

(cation) and phenylpyridine (anion) units. As shown in the crystal structure (Figure 1 and Figures S1 and S2 in the Supporting Information), the resulting 3D supramolecular network devotes approximately 20% of its volume (2108 \AA^3 , the part of the channel included within the unit cell) to host dichloromethane molecules. Two kinds of voids can be detected: large channels and small hydrophobic pockets. The large and isolated channels (876 \AA^3 , the part of the channel included within the unit cell) show an irregular shape with a minimum cross section of $3.5 \times 11.5 \text{ \AA}^2$ and run along the crystallographic c axis. At their largest point, they can accommodate a sphere whose diameter is 5.1 \AA and host eight dichloromethane molecules each. Furthermore, four small and isolated hydrophobic pockets (89 \AA^3 each) host a dichloromethane molecule each. Once the solvent molecules inside the channels are completely eliminated from the framework, the crystallinity decreases, and we cannot ascribe any meaningful cell to the desolvated phase. However, as can be demonstrated by X-ray powder thermodiffraction analysis, the porosity of the material is maintained, since the original phase is easily restored by adding a drop of the proper solvent. This porous network possesses cavities able to host solvent molecules, which can be easily and reversibly removed or substituted. The filling with different solvents can be achieved by dropping solvent onto the powder or suspending the complex salt in the solvent. A study of the uptake of various solvents has been performed; CH_2Cl_2 , amyl acetate (AcOAm), ethyl acetate (AcOEt), diethyl ether, and toluene are rapidly taken up inside the cavities; n -hexane and diisopropyl ether are not entrapped (Figures S3, S4, and S5 in the Supporting Information). As soon as the solvent is removed by vacuum or heating, the process is reverted, and the original desolvated phase is restored (Figure S3 in the Supporting Information). The crystals containing solvent molecules are of better quality and are more transparent (Figure S6 in the Supporting Information). The powder shows selectivity both in absorption and desorption processes, depending on solvent size (Et_2O vs. $i\text{Pr}_2\text{O}$), solvent polarity (AcOEt vs. n -hexane), and the possibility to establish specific interactions with solvent (as in the case of toluene). Indeed, as shown in Figure S5 in the Supporting Information, the loss of solvent in $\mathbf{1} \cdot \text{AcOAm}$ is one order of magnitude slower than in $\mathbf{1} \cdot \text{AcOEt}$, thus confirming that the kinetics of the desolvation process strongly depend on the solvent vapor pressure. However, other more specific factors are at work, such as π stacking. Indeed, the toluene solvate lasts for hours at room temperature, and desolvation only starts at 60°C , whereas the desolvated phase is fully obtained only at 90°C . This behavior opens the possibility to intercalate solvents or small molecules with suitable properties that are able to influence the photophysical properties of the luminescent host.

We have therefore investigated the emission properties of single crystals of the microcrystalline salt in its empty and loaded form. All the spectroscopic measurements on the empty crystals were performed after high-vacuum drying of the crystals with a time- and spectrally resolved confocal microscope (Figure 2a). As mentioned above, complex $\mathbf{1a}$ emits yellow light with a maximum at 564 nm . In contrast, complex $\mathbf{1b}$ emits in the blue-green region with a maximum at

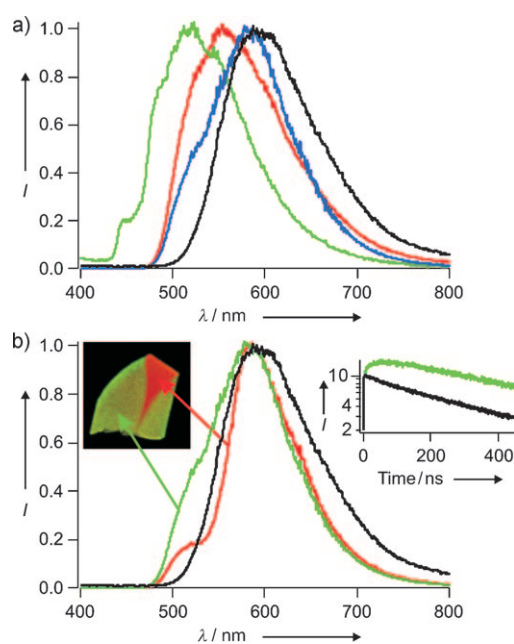


Figure 2. a) Emission spectra of **2** (black empty, blue filled with toluene) and its components (red anionic, green cationic). b) Emission spectra of **2** (black empty) and after immersion in toluene for approximately 1 week (red location with low toluene content, green high toluene content). Insets: dual-color confocal microscopy image of toluene-filled crystal and lifetimes of the red component in empty (black) and toluene-filled crystals (green).

502 nm . When the solvent is removed, the crystal of **1** emits at 591 nm (Figure S7, for lifetime decays see Figure S8 in the Supporting Information), and the emission is uniform in the entire crystal and is quite reproducible for all the crystals. The same behavior is observed for the crystal of **2**. The components emit at 554 nm for **2a** and at 460 nm (shoulder) for **2b**. The crystal **2** emits with a maximum at 596 nm , again well red-shifted compared to the individual components (see Figure 2a, for lifetime decays see Figure S9 in the Supporting Information). It is clear that in the crystalline species an efficient energy transfer takes place from the excited high-energy iridium complex to the lowest excited state located on the yellow-orange-emitting iridium unit (Figure 2a).

However, if the only mechanism present was energy transfer from the blue-green (anionic) species to the yellow-orange (cationic) components, we should observe an emission maxima in the crystals corresponding to that of the component with the lowest excited state: at about 564 nm for **1** and 554 nm for **2**. It is clear, therefore, that another process is occurring, shifting the emission to lower energy.

A close analysis of the packing of the crystals reveals that a strong π - π interaction is present between the complementary iridium components leading, most likely, to a kind of exciplex formation and emission from a correspondingly lower-energy excited state (Figure 2a and Figure S6 in the Supporting Information). In fact, this π - π interaction takes place between the ligands responsible for the lowest excited state of the components (see above). This interaction operates in both types of crystals, since similar packing is expected. Conclusive evidence of such an interaction comes from the

behavior of the emission upon insertion of solvent molecules inside the channels, which can cause a decrease in the π - π interaction by an expansion of the distance between the iridium complexes.

This phenomenon has been monitored for the diffusion of toluene molecules inside the pores of **2**, which causes a blue shift of the emission and slight elongation of the excited-state lifetimes. Figure 2b shows the change in the emission upon diffusion of the toluene molecules in the crystal and the excited-state lifetimes recorded both in the green and in the red region of the spectrum. The decay in the case of toluene encapsulation is also accompanied by a rise time in the excited-state lifetimes recorded in the red region. This effect can be attributed to the fact that the crystal expands to accommodate the solvent, and the two components are at a larger distance, thus decreasing the electronic interaction between the two chromophores, and, more importantly, reducing the probability for the formation of the low-lying excited state that is responsible for the red emission in the crystal. The decrease of such an interaction and associated energy pathway leads to a shift to the blue and reveals the energy transfer process from the **2b** to **2a** units. The rate of such a process ($k_{ET} = 3.27 \times 10^7 \text{ s}^{-1}$) is calculated from the rise time, which is in good agreement with the quenched excited-state lifetime of the blue component $\tau = 28 \text{ ns}$. The change in color of the emission of the crystal can be modulated by the host molecules inserted in the pores of the crystals. We have selected, therefore, a host molecule able to almost selectively quench the iridium complex emitting at lower energy by an efficient photoinduced electron transfer.

A good candidate for such a process is anthraquinone, which can be encapsulated by gas-phase insertion. Anthraquinone can in fact quench, by photoinduced bimolecular electron transfer, the $[\text{Ir}(\text{ppy})_2(\text{bpy})]^+$ (**2a**) excited state, that is, the red component of the crystal **2**, which has a lower oxidation potential (0.92 V) than the blue component (**2b**, 1.46 V). The photoinduced electron-transfer process results in an exergonic reaction ($\Delta G = -0.51 \text{ eV}$), thus leading to oxidized **2a** and reduced anthraquinone (see the Supporting Information for details). As shown in Figure 3, the emission spectrum of the crystal is strongly blue-shifted upon insertion of the guest molecules owing to the quenching of the red component. The emission quenching is accompanied by a

reduction in the excited-state lifetime of the red component from 475 to 72 ns (see Figure S10 in the Supporting Information). The change in color is so dramatic that even with naked eye it is easily seen that upon insertion of anthraquinone the crystal emission changes from yellow-orange to green (Figure 3).

We have demonstrated for the first time that luminescent complexes of complementary colors and charges can be used for the creation of a new class of noncovalently bound porous materials and that their properties depend strongly on intermolecular interactions and on the guests entrapped in their networks. The possibility to modulate reversibly the emission properties by intercalation of small molecules has been illustrated. This discovery could be extended to several classes of electro- and photoresponsive materials, and the selective quenching or enhancement of one of the component's properties opens fascinating routes for the realization of light modulators and novel molecular devices.

Received: October 11, 2009

Published online: January 13, 2010

Keywords: electron transfer · iridium · luminescence · porous materials · supramolecular interactions

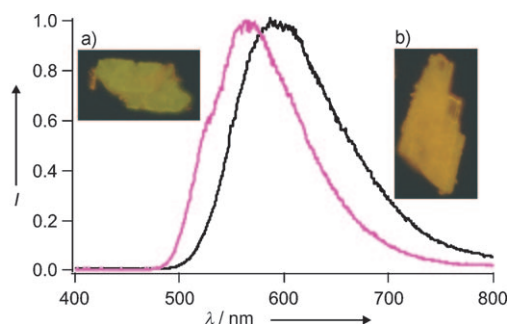


Figure 3. Spectra of compound **2** with anthraquinone loading (magenta) and empty (black). Insets show fluorescence microscopy pictures of a filled crystal (a) and an empty crystal (b).

- [1] M. A. Baldo, D. F. O'Brien, Y. You, A. Shoustitov, S. Sibley, M. E. Thompson, S. R. Forrest, *Nature* **1998**, 395, 151–154.
- [2] S. Lamansky, P. Djurovich, D. Murphy, F. Abdel-Razzaq, H.-E. Lee, C. Adachi, P. E. Burrows, S. R. Forrest, M. E. Thompson, *J. Am. Chem. Soc.* **2001**, 123, 4304–4312.
- [3] A. B. Tamayo, B. D. Alleyne, P. I. Djurovich, S. Lamansky, I. Tsyba, N. N. Ho, R. Bau, M. E. Thompson, *J. Am. Chem. Soc.* **2003**, 125, 7377–7387.
- [4] W.-S. Huang, J. T. Lin, C. H. Chien, Y.-T. Tao, S.-S. Sun, Y.-S. Wen, *Chem. Mater.* **2004**, 16, 2480–2488.
- [5] P. Coppo, E. A. Plummer, L. De Cola, *Chem. Commun.* **2004**, 1774–1775.
- [6] L. Yang, F. Okuda, K. Kobayashi, K. Nozaki, Y. Tanabe, Y. Ishii, M.-A. Haga, *Inorg. Chem.* **2008**, 47, 7154–7165.
- [7] J. Li, P. I. Djurovich, B. D. Alleyne, M. Yousufuddin, N. N. Ho, J. C. Thomas, J. C. Peters, R. Bau, M. E. Thompson, *Inorg. Chem.* **2005**, 44, 1713–1727.
- [8] M. S. Lowry, S. Bernhard, *Chem. Eur. J.* **2006**, 12, 7970–7977.
- [9] M. S. Lowry, W. R. Hudson, R. A. Pascal, S. Bernhard, *J. Am. Chem. Soc.* **2004**, 126, 14129–14135.
- [10] E. Orselli, G. S. Kottas, A. E. Konradsson, P. Coppo, R. Fröhlich, L. De Cola, A. van Dijken, M. Büchel, H. Börner, *Inorg. Chem.* **2007**, 46, 11082–11093.
- [11] D. Di Censo, S. Fantacci, F. De Angelis, C. Klein, N. Evans, K. Kalyanasundaram, H. J. Bolink, M. Grätzel, Md. K. Nazeeruddin, *Inorg. Chem.* **2008**, 47, 980–989.
- [12] Md. K. Nazeeruddin, R. T. Wegh, Z. Zhou, C. Klein, Q. Wang, F. De Angelis, S. Fantacci, M. Grätzel, *Inorg. Chem.* **2006**, 45, 9245–9250.
- [13] C.-H. Yang, Y. M. Cheng, Y. Chi, C. J. Hsu, F.-C. Fang, K.-T. Wong, P.-T. Chou, C.-H. Chang, M.-H. Tsai, C.-C. Wu, *Angew. Chem.* **2007**, 119, 2470–2473; *Angew. Chem. Int. Ed.* **2007**, 46, 2418–2421.
- [14] J. D. Slinker, A. A. Gorodetsky, M. S. Lowry, J. Wang, S. Parker, R. Rohl, S. Bernhard, G. G. Malliaras, *J. Am. Chem. Soc.* **2004**, 126, 2763–2767.
- [15] Y. Sun, N. C. Giebinik, H. Kanno, B. Ma, M. E. Thompson, S. R. Forrest, *Nature* **2006**, 440, 908–912.

- [16] S. Reineke, F. Linder, G. Schwartz, N. Seidler, K. Walzer, B. Lüssem, K. Leo, *Nature* **2009**, 459, 234–239.
- [17] X. Gong, S. Wang, D. Moses, G. C. Bazan, A. J. Heeger, *Adv. Mater.* **2005**, 17, 2053–2058.
- [18] F. Lafolet, S. Welter, Z. Popović, L. De Cola, *J. Mater. Chem.* **2005**, 15, 2820–2828.
- [19] P. Coppo, M. Duati, V. N. Kozhevnikov, J. W. Hofstra, L. De Cola, *Angew. Chem.* **2005**, 117, 1840–1844; *Angew. Chem. Int. Ed.* **2005**, 44, 1806–1810.
- [20] I. M. Dixon, J.-P. Collin, J.-P. Sauvage, L. Flamigni, S. Encinas, F. Barigelletti, *Chem. Soc. Rev.* **2000**, 29, 385–391.
- [21] S. Inagaki, S. Guan, T. Ohsuna, O. Terasaki, *Nature* **2002**, 416, 304–307.
- [22] F. Hoffmann, M. Cornelius, J. Morell, M. Fröba, *Angew. Chem.* **2006**, 118, 3290–3328; *Angew. Chem. Int. Ed.* **2006**, 45, 3216–3251.
- [23] D. J. Tranchemontagne, J. L. Mendosa-Cortés, M. O’Keeffe, O. M. Yaghi, *Chem. Soc. Rev.* **2009**, 38, 1257–1283.
- [24] M. D. Allendorf, C. A. Bauer, R. K. Bhakta, R. J. T. Houk, *Chem. Soc. Rev.* **2009**, 38, 1330–1352.
- [25] D. Zacher, O. Shekhan, C. Wöll, R. A. Fischer, *Chem. Soc. Rev.* **2009**, 38, 1418–1429.
- [26] M. W. Hosseini, *Acc. Chem. Res.* **2005**, 38, 313–323.
- [27] Z. Popović, M. Busby, S. Huber, G. Calzaferri, L. De Cola, *Angew. Chem.* **2007**, 119, 9056–9060; *Angew. Chem. Int. Ed.* **2007**, 46, 8898–8902.
- [28] G. Calzaferri, S. Huber, H. Maas, C. Minkowski, *Angew. Chem.* **2003**, 115, 3860–3888; *Angew. Chem. Int. Ed.* **2003**, 42, 3732–3758.
- [29] The photophysical properties in solution will be reported elsewhere.
- [30] Crystal data for $1^{-1/2}\text{H}_2\text{O}\cdot 2^{1/2}\text{CH}_2\text{Cl}_2$: $\text{C}_{58.5}\text{H}_{42}\text{Cl}_5\text{F}_4\text{Ir}_2\text{N}_8\text{O}_{0.5}$, $M_r = 1502.65$, monoclinic, space group $C2/c$, $a = 22.923(3)$, $b = 34.459(4)$, $c = 16.392(2)$ Å, $\beta = 123.88(2)^\circ$, $V = 10750(3)$ Å³, $Z = 8$, $d_{\text{calc}} = 1.857$ g cm⁻³, $T = 100(2)$ K, crystal size = $0.15 \times 0.13 \times 0.10$ mm³, $\mu = 5.259$ mm⁻¹, $\lambda = 0.71073$ Å. Refinement of 727 parameters on 10555 independent reflections out of 41133 measured reflections ($R_{\text{int}} = 0.0789$, $R_o = 0.0738$, $2\theta_{\text{max}} = 52.0^\circ$) led to $R_1 = 0.0476$ ($I > 2\sigma(I)$), $wR_2 = 0.1284$ (all data), and $S = 1.076$, with the largest peak and hole of 3.224 and -2.300 e Å⁻³. CCDC 722387 ($1^{-1/2}\text{H}_2\text{O}\cdot 2^{1/2}\text{CH}_2\text{Cl}_2$) contains the supplementary crystallographic data for this paper. These data can be obtained free of charge from The Cambridge Crystallographic Data Centre via www.ccdc.cam.ac.uk/data_request/cif.